Multiple-Relay Aided Distributed Turbo Coding Assisted Differential Unitary Space-Time Spreading for Asynchronous Cooperative Networks

S. Sugiura, S. X. Ng, L. Kong, S. Chen and L. Hanzo

School of ECS, University of Southampton, SO17 1BJ, UK, Tel: +44-23-8059-3125, Fax: +44-23-8059-4508

Email: {ss07r,sxn,lk06r,sqc,lh}@ecs.soton.ac.uk, http://www-mobile.ecs.soton.ac.uk

***Abstract*—This paper proposes a cooperative space-time coding (STC) protocol, amalgamating the concepts of asynchronous cooperation, non-coherent detection as well as Distributed Turbo Coding (DTC), where neither symbol-level time synchronization nor CSI estimation is required at any of the cooperating nodes, while attaining a high performance even at low SNRs. More specifically, a practical cooperative differential space-time spreading (CDSTS) scheme is designed with the aid of interference rejection spreading codes, in order to eliminate the effect of synchronization errors between the relay nodes without the assistance of channel estimation or equalization. Furthermore, a set of space-time codewords are constructed based on Differential Linear Dispersion Codes (DLDC), which allows our CDSTS system to support an arbitrary number of relay nodes operating at a high transmission rate due to its flexible design. Rather than using conventional single-relay-assisted DTCs, novel multi-relay-assisted DTCs and a three-stage iteratively-decoded destination receiver structure are developed. In our simulations the system parameters are designed with the aid of EXIT chart analysis, followed by the characterization of the achievable BER performance for various synchronization delay values as well as for various diversity-multiplexing relationships in frequency-selective fast and/or quasi-static Rayleigh fading environments.**

I. Introduction

In recent years, cooperative Space-Time Coding (STC) schemes [1] were proposed, where a collection of single-antenna-aided nodes act as a virtual antenna array, having widely separated distributed antenna elements. Additionally, several cooperative differential STC (CDSTC) schemes [2], [3] have been developed. Since it is a challenging task to acquire accurate Channel State Information (CSI) for both the source-relay (SR) and/or for the relay-destination (RD) links for a rapidly changing topology of vehicles, in recent years non-coherent detection techniques attracted substantial attention.

On the other hand, most of the previous cooperative STC schemes [1]–[3] have exploited the assumption of perfect symbol timing synchronization between the cooperating nodes, which is typically an unrealistic assumption, considering the rapidly changing topology of the relay nodes. Since the resultant time synchronization errors impose a significant performance degradation as noted in [4], asynchronous cooperation schemes were investigated in [5], [6], under the assumption of having perfect CSI and/or delay information at the destination node. More recently, a CDSTC scheme was proposed for realistic asynchronous relay networks in [7] with the aid of interference rejection spreading codes, namely Loosely Synchronous (LS) codes [8], in order to achieve a useful cooperative space-time diversity gain without symbol-level time synchronization or CSI estimation at any of the nodes.

Moreover, the Distributed Turbo Coding (DTC) philosophy was presented in [9], [10], where the turbo coding principle [11] was applied to a single-relay-assisted cooperative system. Whilst in general cooperative STCs have the capability of achieving the maximum attainable diversity order in the high SNR regime, the DTC aims for achieving an additional *turbo processing gain*, and therefore it is particularly suitable for operation at low SNRs. Here we note that most of the previous DTC schemes proposed in the open literature [9], [10] are based on a two-stage parallel-concatenated arrangement assisted by a single relay node, assuming that there is a perfect link between the cooperating nodes. More recently, a sophisticated three-component DTC scheme was proposed in [12], also assuming the assistance of a single relay node.

Against this background, the main contributions of this paper are as follows. Motivated by the concept of [7], we first present a cooperative STC protocol, amalgamating the concepts of asynchronous cooperation as well as of non-coherent detection, where a multi-relay-assisted three-stage DTC is employed, unlike the family of conventional single-relay-assisted DTCs [9], [10], [12]. Furthermore, STC blocks of our CDSTS are constructed based on Differential Linear Dispersion Codes (DLDCs) [13], which have the capability of striking a flexible diversity versus multiplexing tradeoff and hence of adapting our CDSTS arrangement, depending on the number of relay nodes as well as on the target transmission rate.

II. System Overview

Consider a Time Division-Code Division Multiple Access (TD-CDMA) based channel allocation scheme supporting $(N_{\rm T} \times N_{\rm C})$ source nodes, namely supporting $N_{\rm C}$ source nodes in each of the $N_{\rm T}$ time slots. Here, it is assumed that each node has a node-specific synchronization delay, uniformly distributed from 0 to $\tau_{\max}$, where $\tau_{\max}$ denotes the maximum delay. Each source node transmits its signals to the destination node(s) with the aid of the source-specific relay nodes selected from the other source nodes. More specifically, each transmission is composed of two phases, i.e. a broadcast phase-I and a cooperative phase-II. Additionally, we assume that a unity total power is shared by the collaborating nodes, where the power values $P_{\rm S}$ and $P_{\rm R}$ are allocated to the source node and the corresponding M relay nodes, respectively, while maintaining the relation of $P_{\rm S} + P_{\rm R} = 1$. In this paper, we set $P_{\rm S} = P_{\rm R} = 0.5$, as suggested in [3].

The financial support of the EU under the auspices of the Optimix project and of the EPSRC UK is gratefully acknowledged. The work of S. Sugiura was sponsored in part by the Toyota Central Research & Development Laboratories, Inc.

978-1-4244-2519-8/10/$26.00 ©2010 IEEE

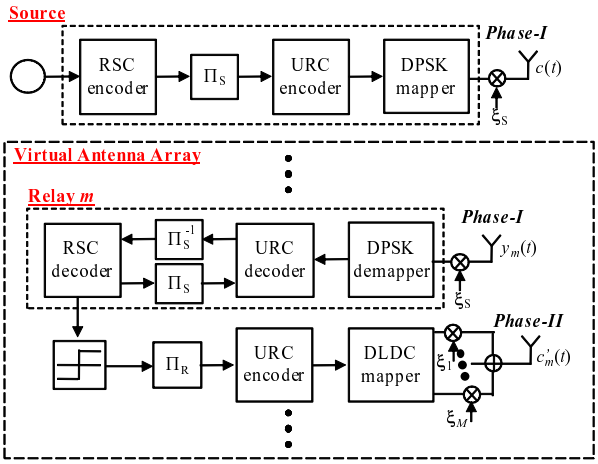

Fig. 1. Schematic of the source and relay nodes.

For simplicity of treatment, we in the rest of this section focus our attention on each of the $N_{\rm C}$ in different transmissions taking place in a certain time slot, indicating that we ignore the interference between the source and relay nodes allocated to the same time slot. During our later discourse Section V and Section VI will then develop our scheme further by taking into account the effect of the Multi-User Interference (MUI) imposed. Furthermore, let us define $d_{\rm sd}$, $d_{\rm sr}$ and $d_{\rm rd}$, as the average geometrical distances of the source-destination link, of the source-relay links and of the relay-destination links, respectively. Here, each path-loss value of the corresponding links can be modeled by $P({\rm ab}) = K \cdot d_{\rm ab}^{-\alpha}$ $({\rm a,b = s,d,r})$, where K is the constant element and α is the path loss exponent. Considering a free-space propagation model of $\alpha = 2$, the power gain $G_{\rm sr}$ of the source-relay link and that of the relay-destination link $G_{\rm rd}$ over the source-destination link is given by $G_{\rm sr} = (d_{\rm sd}/d_{\rm sr})^2$ and $G_{\rm rd} = (d_{\rm sd}/d_{\rm rd})^2$, respectively.

A. Source Model

During the broadcast phase-I, the source node transmits its differentially-encoded signals to the corresponding M relay nodes as well as to the destination node. As shown in the top part of Fig. 1, the source node first channel-encodes the source bits $b(i)$ with the aid of a half-rate Recursive Systematic Convolutional (RSC) code, and then interleaves the channel-encoded bits by using the source-specific interleaver $\Pi_{\rm S}$. Furthermore, the interleaved bits are further encoded by a recursive Unity-Rate Code (URC) [14][1] , and then the coded bits are input to the DPSK mapper block. Finally the DPSK-modulated symbols $c(k)$ are spread with the aid of the source-specific direct sequence spreading code $\xi_{\rm S}(t)$, having the code length of $L_{\rm S}$ and the chip durations of $T_{\rm c}$. Under the condition of frequency-selective Rayleigh fading channels having a maximum number of resolvable paths $L_{\rm p}$, the time-domain signals $y_m(t)$ received at the mth relay node and the destination node $y_{\rm sd}(t)$ are expressed, respectively, as

[1]The role of the URC is to impose an Infinite Impulse Response (IIR), which improves the achievable iterative decoding performance by efficiently spreading the extrinsic information, as detailed in [15].

$$y_m(t) = \sqrt{P_{\rm S} G_{\rm sr}} \sum_{k=0}^{N_{\rm M}-1} \sum_{l=1}^{L_{\rm p}} h_{{\rm sr}_m}^{(l)} c(k) \xi_{\rm S}(t - kL_{\rm S}T_{\rm c}) + n_m(t) \quad (1)$$

$$y_{\rm sd}(t) = \sqrt{P_{\rm S}} \sum_{k=0}^{N_{\rm M}-1} \sum_{l=1}^{L_{\rm p}} h_{\rm sd}^{(l)} c(k) \xi_{\rm S}(t - kL_{\rm S}T_{\rm c}) + n_{\rm d}(t), \quad (2)$$

where $h_{{\rm sr}_m}^{(l)}$ and $h_{\rm sd}^{(l)}$ are the corresponding Rayleigh fading coefficients associated with the lth path, while n_m and $n_{\rm d}$ are the noise components having a zero mean and a variance of $N_0/2$ per dimension. Furthermore, $N_{\rm M}$ indicates the number of modulated symbols. Here, the SNRs at the relay nodes, namely ${\rm SNR}_{\rm sr}$, and at the destination node ${\rm SNR}_{\rm sd}$ have the relation of ${\rm SNR}_{\rm sr} = {\rm SNR}_{\rm sd} + 10\log_{10}(G_{\rm sr})$ expressed in dB due to the geometrical power-gain effect [12]. Furthermore, the transmission rate of the phase-I $R_{\rm S}$ is given by $R_{\rm S} = \frac{r}{2}$ bits/symbol, where r is the number of bits/symbol for the DPSK modulation scheme employed.

B. Relay Model

During the cooperative phase-II, the M relay nodes implement the decode-and-forward CDSTC transmission scheme based on the DLDC-coded STS concept, where each of the M relay nodes use all the M spreading codes according to the DSTS principle [15]. The M spreading codes have a code length of $L_{\rm R}$. Letting the mth relay node be the node of interest, the received signals $y_m(t)$ are first despread by the source node's spreading code $\xi_{\rm S}(t)$, and then iteratively decoded according to the turbo principle [11]. Next, the estimated bits $\hat{b}(i)$ are interleaved and coded by the interleaver $\Pi_{\rm R}$ and the URC encoder, which are common for the associated M relay nodes. Then, the coded bits are mapped to DLDC blocks [13], which is represented by $\boldsymbol{S}^{(k)} = [s_{ij}^{(k)}] \in \mathcal{C}^{M \times M}$, where $s_{ij}^{(k)}$ indicates the ith-row and jth-column element of the codeword $\boldsymbol{S}^{(k)}$ and k is the block index. Here, Q BPSK symbols are multiplexed in each of the codewords $\boldsymbol{S}^{(k)}$. It should be emphasized that the DLDC has the capability of striking a balance between the attainable diversity and multiplexing gain [15], enabling us to generate a set of M codewords while having a multiplexing order Q, without exhibiting a substantial information rate loss in comparison to the theoretical upper bound. This high degree of freedom enables the flexible adjustment of the number of cooperating relay nodes and the resultant phase-II throughput, depending on the rate of change in the network topology and the propagation environment.

Instead of arranging for each relay node to transmit each row of the DLDC codeword $\boldsymbol{S}^{(k)}$ during M symbol durations in the conventional way [1], here we apply the concept of STS [15] during the phase-II transmissions with the aid of the M spreading codes seen in Fig. 1. This operation assists the destination receiver to rearrange the received DLDC space-time codeword, hence eliminating the effect of synchronization errors between the relay nodes, provided that the spreading sequences have ideal cross-correlation properties. To be specific, the mth relay node spreads each component of the mth row in $\boldsymbol{S}^{(k)}$ with the aid of a different spreading code for each component, and transmits the linear combination of the spread symbols in a concerted action with the other relay nodes, as

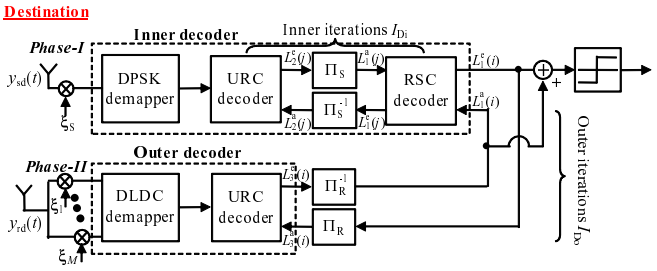

Fig. 2. The three-stage iterative detector at the destination node.

closely synchronized as possible.[2] Therefore, the time-domain signals $y_{\rm rd}(t)$ received at the destination node during phase-I I of Fig. 1 is represented by

$$y_{\rm rd}(t) = \sqrt{\frac{P_{\rm R}G_{\rm rd}}{M}} \sum_{k=0}^{N_{\rm B}-1} \sum_{l=1}^{L_{\rm P}} \sum_{m=1}^{M} \sum_{j=1}^{M} h_{{\rm rd}_m}^{(l)} s_{m,j}^{(k)} \times \xi_j(t - kL_{\rm R}T_{\rm c} - \tau_{m,l}) + n_{\rm d}(t), \quad (3)$$

where $h_{{\rm rd}_m}^{(l)}$ is the Rayleigh channel coefficient between the mth relay node and the destination node, associated with the lth path, while $\tau_{m,l}$ is the delay component corresponding to the mth user and the lth path. Furthermore, $\xi_j(t)$ is the normalized signature sequence of the jth spreading code. Note that the corresponding transmission rate $R_{\rm R}$ of phase-Ⅱ is given by $R_{\rm R} = Q$ bits/symbol. Similarly to the source-relay SNR of $\text{SNR}_{\rm sr}$, the relay-destination SNR of $\text{SNR}_{\rm rd}$ and the source-destination SNR of $\text{SNR}_{\rm sd}$ have the relation of $\text{SNR}_{\rm rd}$ = $\text{SNR}_{\rm sd}$ + $10\log_{10}(P_{\rm R}G_{\rm rd}/P_{\rm S})$ in dB. At the destination node, the source bits are iteratively detected based on the signals $y_{\rm sd}(t)$ in (2) received during phase-I as well as the signals $y_{\rm rd}(t)$ in (3) received during phase-Ⅱ, which will be detailed in the following section.

III. Three-Stage Iterative CDSTS Detector Structure

In this section, we present the destination receiver's structure for our CDSTS scheme, where a three-stage iterative decoding algorithm is employed, as illustrated in Fig. 2. For ease of treatment we refer to the DPSK demapper, the URC decoder and the RSC decoder of phase-I as an *inner decoder*, while the DLDC demapper and the URC decoder of phase-Ⅱ are considered as an *outer decoder*. To be specific, the Soft-Input Soft-Output (SISO) decoders at the receiver iteratively exchange soft extrinsic information L_i^e in the form of Log Likelihood Ratios (LLRs). At the *inner decoder* of Fig. 2, the destination receiver decodes the signals broadcast from the source node during phase-I, in order to output the extrinsic LLR $L_1^e(i)$. The same procedure is followed by the relays' iterative decoders seen in Fig. 1, with the sole difference that the RSC decoder block of the above-mentioned *inner decoder* can make use of the *apriori* information $L_1^a(i)$ gleaned from the *outer decoder*. The number of inner iterations between the two decoders within the *inner decoder* is represented by $I_{\rm Di}$.

[2]To elaborate a little further, the cooperative phase of our CDSTS scheme requires M different spreading sequences and a signle symbol duration per block, while that of the conventional cooperative STC uses only one spreading sequence and M symbol durations per block.

By contrast, at the *outer decoder* of Fig. 2, the destination receiver first despreads the signals, which are received during phase-Ⅱ. We note here that at this despreading stage the effects of the synchronization errors between the relay nodes are eliminated. Then, the DLDC demapper produces soft information, where a conventional linear MIMO decoder [15], [16] can be employed due to the linearization operation of [13]. Then, the resultant soft information is input to the URC decoder of Fig. 1 in order to output the extrinsic LLR $L_3^e(i)$ of the *outer decoder*. Furthermore, the soft LLRs are iteratively exchanged between the *inner decoder* and the *outer decoder*, where the associated number of outer iterations is denoted as $I_{\rm Do}$. Note that in this three-stage iterative decoding process, the total number of iterations is given by $(I_{\rm Di} \times I_{\rm Do})$. Finally, the estimated bits are calculated from the LLRs $L_1^a(i)$ and $L_1^e(i)$ with the aid of the hard-decision operation.

IV. Interference Rejection Spreading Codes

In our CDSTS scheme the effects of asynchronous relay nodes are eliminated under the ideal assumption that the despreading operation at the destination receiver is capable of sufficiently suppressing both the asynchronous MUI as well as the multi-path-induced Inter-Symbol Interference (ISI). This indicates that low cross-correlations as well as auto-correlations are required for the spreading codes employed. However, the conventional spreading codes, such as Walsh codes and Gold codes, normally suffer from both MUI and from MultiPath Interference (MPI) due to the non-negligible auto- and/or cross-correlation values. To this end, we employ here the above-mentioned LS codes as the spreading codes in our CDSTS system, according to the proposal in [7]. The family of LS codes exhibits a so-called Interference-Free Window (IFW), resulting in zero ISI and zero Multiple-Access Interference (MAI), provided that the maximum delay of the asynchronous transmissions including all MPI components is within the width of the IFW. As detailed in [8], the parameter-based notation of LS codes is given by LS($N_{\rm LS}$, $P_{\rm LS}$, W_0), where $N_{\rm LS}$ is the length of the constituent orthogonal complementary code set, $P_{\rm LS}$ is the dimension of the Walsh-Hadamard matrix used for generating members of the code-family and W_0 is the width of the IFW, which are used to design the desired LS code. As a result, we can generate $P_{\rm LS}$ LS codes having an IFW of at least $\min\{N_{\rm LS}-1, W_0\}$ chip durations, where the corresponding code length of the LS codes is $L = N_{\rm LS}P_{\rm LS} + 2W_0$. Owing to space-limitations, the detailed method of creating the LS code is omitted, which is available in [8].

V. EXIT chart analysis

In this section we investigate the effects of diverse system parameters on our CDSTS system with the aid of EXIT charts. Here, the number of source nodes allocated to each time slot is set to $N_{\rm C} = 4$. Let us define here the equivalent transmit SNR ρ as $\rho = (P_{\rm S} + P_{\rm R})/N_0$, which relates the total source-power $P_{\rm S}$ plus relay-power $P_{\rm R}$ to the noise-power N_0 at the receiver. Additionally, we consider frequency-selective block-fading Rayleigh channels, where the channel coefficients can be regarded as constant during two DLDC block durations,

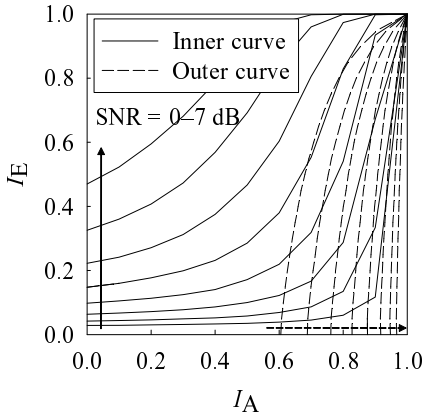

Fig. 3. The EXIT curves of the *inner decoder* and *outer decoders* of our CDSTS system seen in Fig. 2, supporting N_C = 4 source nodes in each time slot and employing DQPSK modulation at each source nodes and DLDC's multiplexing factor of Q = 2 at the corresponding M = 2 relay nodes. The equivalent transmit SNR was varied from SNR = 0 dB to 7 dB, while the maximum synchronization delay was $\tau_{\max} = 3T_c$.

while the number of resolvable paths L_p as well as the number of RAKE combiner fingers ν is four.

First, we investigated the decoding characteristics of the destination receiver of Fig. 2 in our CDSTS system, where each source node was assisted by M = 2 relay nodes and Q = 2 BPSK symbols were multiplexed per each DLDC codeword. We assumed that the each node's geometrical relationship, defined in Section II, was given by $G_{sr} = 8$ and $G_{rd} = 2$. Furthermore, the LS(8,4,7) and LS(8,8,7) codes were preassigned for the source and relay nodes, respectively. Fig. 3 shows the EXIT curves of both the *inner decoder* and of the *outer decoder*, where the transmit SNR was varied from SNR = 0 dB to 7 dB in 1 dB steps, while satisfying the maximum synchronization delay range of $\tau_{\max} = 3T_c$. Furthermore, a half-rate RSC code having the octally-represented generator polynomials of (g_r, g) = (7,5)$_8$ was employed as our channel encoder at the source nodes. As we can see from Fig. 3, upon increasing the transmit SNR, the open EXIT tunnel between the EXIT cuves of the *inner* and *outer decoders* becomes wider, potentially leading to a fast convergence of the iterative process.

VI. Performance Results

In this section we provide performance results for the CDSTS system. The basic system parameters employed in our simulations are listed in Table I, which we derived with the aid of our EXIT chart analysis of the previous section. A DQPSK modulation scheme and an interleaver Π_S having the length of 20 000 bits were employed at the N_C source nodes, each of which was assisted by $M = 2$ relay nodes employing a DLDC multiplexing factor of $Q = 2$ and an interleaver Π_S having a length of 10 000 bits. The number of iterations at each relay node I_R was set to $I_R = 2$, while the number of inner and outer iterations at the destination node was given by $I_{Di} = 2$ and $I_{Do} = 5$, respectively. Furthermore, the maximum synchronization delay $\tau_{\max}$ was set to $\tau_{\max} = 3T_c$.

TABLE I
Basic system parameters

Source node	Number of source nodes per time slot	N_C = 4
	Interleaver block length of Π_S	20 000 bits
	Spreading codes	LS codes of LS(8,4,7)
	Outer channel code	RSC with generator polynomials (7,5)$_8$
	Precoder code	URC $G(D) = 1/(1+D)$ [14]
	Power allocation	P_S = 0.5
Relay node	Number of relay nodes per source node	M = 2
	DLDC's multiplexed factor	Q = 2
	Interleaver block length of Π_R	10 000 bits
	Spreading codes	LS codes of LS(8,8,7)
	Precoder code	URC $G(D) = 1/(1+D)$ [14]
	DPSK demapper	Soft ML detector [11]
	Number of iterations	I_R = 5
	Power gain of SR links	G_{sr} = 8
	Power allocation	P_R = 0.5
Destination	DPSK demapper	Soft ML detector [11]
	DLDC demapper	MMSE-based soft IC [15]
	Number of iterations	(I_{Di},I_{Do}) = (2,5)
	Power gain of RD links	G_{rd} = 2

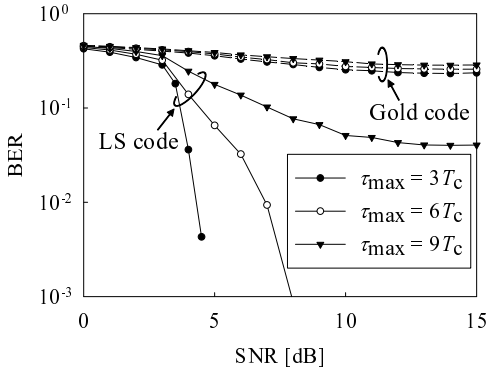

Fig. 4. Achievable BER performance of our LS code-aided and the Gold code-aided CDSTS schemes, comparing the maximum synchronization delays of $\tau_{\max}$=3T_c, 6T_c and 9T_c, while having L_p=4 delay spread-induced paths.

Here, the total transmission rate of our CDSTS R_{total} was given by $R_{total} = L_S / \left(\frac{L_S}{R_S} + \frac{L_R}{R_R}\right)$ [bits/symbol], where L_S and L_R are the code lengths of the spreading codes during phase-I and phase-II, respectively, and the rate R_{total} was normalized by the phase-I code length L_S. Based on these relationships, the transmission rate of our CDSTS was given by R_{total} = 0.54, while for instance that of the DBPSK-modulated non-cooperative scenario was R_S = 0.5.

Fig. 4 shows the achievable BER performance of our LS code-aided and Gold code-aided CDSTS schemes, where the maximum synchronization delays $\tau_{\max}$ were set to $\tau_{\max} = 3T_c$, $6T_c$ and $9T_c$, while having $L_p = 4$ resolvable paths and $\nu = 4$ RAKE combiner fingers. It can be seen from Fig. 4 that the BER curve of our LS code-based CDSTS system recorded for the case of $\tau_{\max} = 3T_c$ exhibited a good BER performance, as expected on the basis of the EXIT chart analysis of Fig. 3 in the previous section. On the other hand, for the high-delay scenarios of $\tau_{\max} = 6T_c$ and $9T_c$, where the sum of the maximum delay $\tau_{\max}$ and the delay spread (L_p–1) is higher than the LS code's IFW, the corresponding BER was substantially deteriorated due to the residual MUIs and MPIs, although it was still better than that of the Gold codes for any

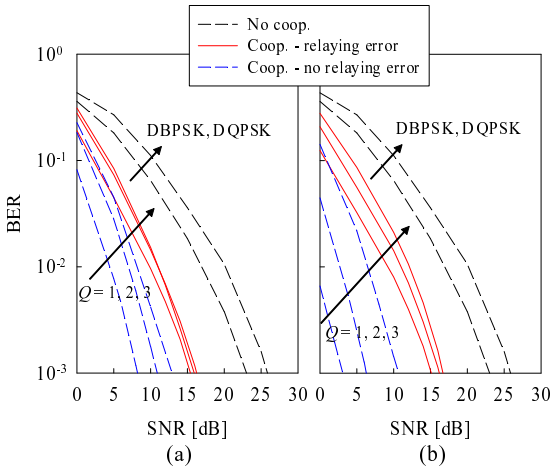

Fig. 5. Achievable BER performance of our LS code-aided CDSTS scheme, employing (a) $M = 2$ and (b) $M = 3$ cooperating nodes for each source node, where the DLDC's multiplexing factor Q is changed from $Q = 1$ to $Q = 3$. We also plotted here the corresponding BER curves of our system suffering from no relaying errors, as well as those of non-cooperative system having the modulations of DBPSK and DQPSK.

of the delays considered.

Finally, we investigated a more practical scenario, namely that of employing the shorter interleaver lengths of Π_S=2 000 bits and of Π_R=1 000 bits. Here we assumed quasi-static Rayleigh fading environments. Furthermore, the LS code of LS(8,16,7) was employed for the case of M=3 relay nodes, in order to generate the required number of LS codes having an IFW of 7 chip durations. It is predicted that since no *time diversity gain* can be exploited in this block-fading scenario, the spatial diversity order, determined by the number of relay nodes dominantly affects the attainable performance improvement. Hence our multi-relay-assisted DTC has the potential to exhibit a better performance than those of the conventional single-relay-assisted DTCs [9], [10], [12]. Figs. 5(a) and 5(b) show the achievable BER performance of our LS code-aided CDSTS scheme, employing M=2 and M=3 cooperating nodes, respectively, where the DLDC's multiplexing factor Q was varied from Q=1 to Q=3. Additionally, we plotted here the BER curves of our benchmark CDSTS system assuming the idealized scenario of having no decoding errors at the relay nodes, in order to benchmark the effects of the relays' decoding errors and their error propagation. Observe in both Figs. 5(a) and 5(b) that while the proposed CDSTS system achieved a better performance than the non-cooperative scheme as a benefit of its cooperative spatial diversity gain, it was severely degraded by the relays' decoding errors, when compared to those of the no-relaying error scenario. Therefore, it was found that in order to exploit the designed diversity-multiplexing tradeoff, it is important to overcome the effects of error propagation by employing Cyclic Redundancy Checks (CRC) for the sake of identifying the relays' decoding errors, or by introducing the concept of [17], where the relays' decoding errors are compensated for at the destination receiver by exploiting each relay's average BER estimated for the received LLRs.

VII. Conclusions

This paper proposed a practical CDSTC protocol, exploiting the advantages of asynchronous cooperation, non-coherent detection and multi-relay-assisted DTC. The DLDC scheme employed for our STC blocks has the potential of adapting our CDSTS arrangement, such as the number of relay nodes and the transmission rate. Furthermore, according to the distributed turbo coding principle, the three-stage iterative destination receiver structure was designed with the aid of EXIT chart analysis. Our simulation results demonstrated that the proposed LS code-aided CDSTS scheme is capable of both achieving spatial diversity and turbo processing gains aided time-diversity, while combating the effects of the relays' synchronization errors and CSI estimation errors.

References

[1] J. Laneman and G. Wornell, "Distributed space-time-coded protocols for exploiting cooperative diversity in wireless networks," *IEEE Transactions on Information Theory*, vol. 49, no. 10, pp. 2415–2425, 2003.

[2] P. Tarasak, H. Minn, and V. Bhargava, "Differential modulation for two-user cooperative diversity systems," *IEEE Journal on Selected Areas in Communications*, vol. 23, no. 9, pp. 1891–1900, 2005.

[3] Y. Jing and H. Jafarkhani, "Distributed differential space-time coding for wireless relay networks," *IEEE Transactions on Communications*, vol. 56, no. 7, pp. 1092–1100, 2008.

[4] R. C. Palat, A. Annamalai, and J. H. Reed, "Accurate bit-error-rate analysis of bandlimited cooperative OSTBC networks under timing synchronization errors," *IEEE Transactions on Vehicular Technology*, vol. 58, no. 5, pp. 2191–2200, 2009.

[5] X. Li, "Space-time coded multi-transmission among distributed transmitters without perfect synchronization," *IEEE Signal Processing Letters*, vol. 11, no. 12, pp. 948–951, 2004.

[6] Z. Li and X. Xia, "An Alamouti coded OFDM transmission for cooperative systems robust to both timing errors and frequency offsets," *IEEE Transactions on Wireless Communications*, vol. 7, no. 5 Part 2, pp. 1839–1844, 2008.

[7] S. Sugiura, S. Chen, and L. Hanzo, "Cooperative differential space-time spreading for the asynchronous relay aided CDMA uplink using interference rejection spreading code," *IEEE Signal Processing Letters*, vol. 17, no. 2, pp. 117–120, 2010.

[8] L. Hanzo, J. Blogh, and S. Ni, *3G, HSPA and FDD versus TDD Networking: Smart Antennas and Adaptive Modulation*. John Wiley and IEEE Press, 2008, **564 pages**.

[9] B. Zhao and M. Valenti, "Distributed turbo coded diversity for relay channel," *Electronics letters*, vol. 39, p. 786, 2003.

[10] Y. Li, B. Vucetic, T. Wong, and M. Dohler, "Distributed turbo coding with soft information relaying in multihop relay networks," *IEEE Journal on Selected Areas in Communications*, vol. 24, no. 11, pp. 2040–2050, 2006.

[11] L. Hanzo, T. Liew, and B. Yeap, *Turbo Coding, Turbo Equalisation, and Space-Time Coding for Transmission over Fading Channels*. John Wiley and IEEE Press, 2002, **766 pages**.

[12] S. Ng, Y. Li, and L. Hanzo, "Distributed turbo trellis coded modulation for cooperative communications," in *IEEE International Conference on Communications, Dresden, Germany*, June 2009.

[13] B. Hassibi and B. Hochwald, "Cayley differential unitary space-time codes," *IEEE Transactions on Information Theory*, vol. 48, no. 6, pp. 1485–1503, 2002.

[14] D. Divsalar, S. Dolinar, and F. Pollara, "Serial concatenated trellis coded modulation with rate-1 inner code," in *IEEE Global Telecommunications Conference*, vol. 2, San Francisco, CA, November–December 2000, pp. 777–782.

[15] L. Hanzo, O. Alamri, M. El-Hajjar, and N. Wu, *Near-Capacity Multi-Functional MIMO Systems: Sphere-Packing, Iterative Detection and Cooperation*. John Wiley and IEEE Press, 2009, **714 pages**.

[16] S. Sugiura, S. Chen, and L. Hanzo, "Reduced-complexity iterative Markov chain MBER detection for MIMO systems," *IEEE Signal Processing Letters*, vol. 16, no. 3, pp. 160–163, 2009.

[17] K. Lee and L. Hanzo, "Iterative detection and decoding for hard-decision forwarding aided cooperative spatial multiplexing," in *IEEE International Conference on Communications, Dresden, Germany*, June 2009.